



## Chinese herb microneedle patch for wound healing

Junjie Chi<sup>a</sup>, Lingyu Sun<sup>b,d</sup>, Lijun Cai<sup>b,d</sup>, Lu Fan<sup>b,d</sup>, Changmin Shao<sup>a,e,\*</sup>, Luoran Shang<sup>a,c,\*\*</sup>, Yuanjin Zhao<sup>a,b,d,\*\*\*</sup>

<sup>a</sup> Translational Medicine Laboratory, The First Affiliated Hospital of Wenzhou Medical University, Wenzhou, 325035, China

<sup>b</sup> Department of Burns and Plastic Surgery, Nanjing Drum Tower Hospital, The Affiliated Hospital of Nanjing University Medical School, Nanjing, 210008, China

<sup>c</sup> Zhongshan-Xuhui Hospital, The Shanghai Key Laboratory of Medical Epigenetics, Institutes of Biomedical Sciences, Fudan University, Shanghai, 200032, China

<sup>d</sup> State Key Laboratory of Bioelectronics, School of Biological Science and Medical Engineering, Southeast University, Nanjing, 210096, China

<sup>e</sup> Wenzhou Institute, University of Chinese Academy of Sciences, Wenzhou, Zhejiang, 325001, China

### ARTICLE INFO

#### Keywords:

Chinese herb  
Microneedle  
Asiatic acid  
Wound healing  
Patch

### ABSTRACT

Traditional Chinese medicine and Chinese herbs have a demonstrated value for disease therapy and sub-health improvement. Attempts in this area tend to develop new forms to make their applications more convenient and wider. Here, we propose a novel Chinese herb microneedle (CHMN) patch by integrating the herbal extracts, *Premna microphylla* and *Centella asiatica*, with microstructure of microneedle for wound healing. Such path is composed of sap extracted from the herbal leaves via traditional kneading method and solidified by plant ash derived from the brine induced process of tofu in a well-designed mold. Because the leaves of the *Premna microphylla* are rich in pectin and various amino acids, the CHMN could be imparted with medicinal efficacy of heat clearing, detoxicating, detumescence and hemostatic. Besides, with the excellent pharmaceutical activity of Asiatic acid extracted from *Centella asiatica*, the CHMN is potential in promoting relevant growth factor genes expression in fibroblasts and showing excellent performance in anti-oxidant, anti-inflammatory and anti-bacterial activity. Taking advantages of these pure herbal compositions, we have demonstrated that the derived CHMN was with dramatical achievement in anti-bacteria, inhibiting inflammatory, collagen deposition, angiogenesis and tissue reconstruction during the wound closure. These results indicate that the integration of traditional Chinese herbs with progressive technologies will facilitate the development and promotion of traditional Chinese medicine in modern society.

### 1. Introduction

Inadvertent bruise or malicious injury by violence usually gives rise to severe damage on skin and forms wounds, which is difficult to heal, or even causes further fatal septicemia after bacterial infection [1–6]. Therefore, wound healing has been regarded as a hot topic both in fundamental research field and in clinical medicine, becoming a grave threat to socioeconomic development around the world [7–11]. Microneedle (MN) patch has been proposed as a versatile technique and gained a great deal of remarkable achievements in the field of wound healing, as well as disease therapy, biosensing, dermal vaccination, and

so on [12–18]. Because of their well-designed microstructures and superior loading capacity compared to those regular drug delivery carriers, MN can effectively realize the load and delivery of the favored active drugs [19–23]. However, the MN widely utilized nowadays is usually fabricated by synthetic polymer materials obtained through complicated chemical synthesis involving environmentally unfriendly organic reagents and harsh experimental treatments, increasing the risk of side effects [24–28]. In addition, the acquisition of the loaded active drugs generally undergoes a period of extremely strict clinical trials and cruel elimination, which restricts the development of MN-based iatrotechnics [29–31]. Thus, a brand-new MN patch integrated with easily

Peer review under responsibility of KeAi Communications Co., Ltd.

\* Corresponding author. Wenzhou Institute, University of Chinese Academy of Sciences, Wenzhou, Zhejiang, 325001, China.

\*\* Corresponding author. Zhongshan-Xuhui Hospital, The Shanghai Key Laboratory of Medical Epigenetics, Institutes of Biomedical Sciences, Fudan University, Shanghai, 200032, China.

\*\*\* Corresponding author. State Key Laboratory of Bioelectronics, School of Biological Science and Medical Engineering, Southeast University, Nanjing, 210096, China.

E-mail addresses: [shaocm@wiucas.ac.cn](mailto:shaocm@wiucas.ac.cn) (C. Shao), [luoranshang@fudan.edu.cn](mailto:luoranshang@fudan.edu.cn) (L. Shang), [yjzhao@seu.edu.cn](mailto:yjzhao@seu.edu.cn) (Y. Zhao).

<https://doi.org/10.1016/j.bioactmat.2021.03.023>

Received 14 December 2020; Received in revised form 10 March 2021; Accepted 10 March 2021

2452-199X/© 2021 The Authors. Publishing services by Elsevier B.V. on behalf of KeAi Communications Co. Ltd. This is an open access article under the CC

BY-NC-ND license (<http://creativecommons.org/licenses/by-nc-nd/4.0/>).

acquired natural drugs that can amicably and effectively realize drug delivery is with increasing expectations for wound healing.

In this work, we propose a novel Chinese herb microneedle (CHMN) patch with the desired features for wound healing, as schemed in Fig. 1. Traditional Chinese medicine (TCM) has been adopted and carried forward for thousands of years. It is considered that over 80% of people in developing countries and even one-third in developed countries adopt herbs to cure diseases such as common cold and chronic diabetes. Also, a great many of studies have shown that TCM as well as many classical formulae exhibit prominent achievements with diabetes, hypertension, cancers, malaria, and so on [32–35]. Thus, TCM based Chinese herbs, the main means of TCM treatment, usually act on multiple targets and possess multilevel functions, earning increasing attention in the fields of disease therapy and sub-health improvement. Although with promising successes, the active ingredients and effective targets of Chinese herbs have been lack of systematic and scientific investigation [36–38]. In addition, traditional administration modes, including directly external application after rough comminution and oral administration through complicated decoction by patients themselves, are incapable of effectively playing the therapeutic effect of Chinese herbs and are severely restricted by the site. These drawbacks that existed since TCM appeared on the stage of human medical history have greatly limited the development and spread of Chinese herbs to a large extent.

Herein, inspired by the processing procedure of tofu, we addressed these limitations by integrating Chinese herbs into MN structure through brine induced solidification to construct a pure CHMN patch in a well-designed mold. As a proof of concept, two kinds of traditional Chinese herbs, *Premna microphylla* and *Centella asiatica* [39–41], were employed as elements of the CHMN patch. Such path was fabricated by sap extracted from their leaves via traditional kneading method and solidified by plant ash. As the leaves of the *Premna microphylla* are rich in pectin and various amino acids, it is usually processed into tofu by simple brine induced solidification (named “Guanyin tofu” in some areas of China) and still retain medicinal efficacies of heat clearing, detoxicating, detumescence, and hemostatic. Besides, the *Centella asiatica* also exhibits superior medicinal efficacy attributed to its extraction, Asiatic acid (AA), which has been certified effective in promoting relevant growth factor genes expression in fibroblasts and showing excellent performance in anti-oxidant, anti-inflammatory, and anti-bacterial activity [42–44]. Taking advantages of these pure herbal compositions, we have demonstrated that the derived CHMN could prominently promote the formation of neovascular, collagen and the granulation tissue during the wound healing. Thus, we believe that the combination of Chinese herbs and microneedles will benefit in the

development and promotion of Chinese herbs and TCM around the world.

## 2. Experimental section

### 2.1. Materials and animals

Asiatic acid ( $\geq 98\%$  (HPLC), from *Centella asiatica*), poly (ethylene glycol) diacrylate (average Mn 700) (PEGDA), 2-Hydroxy-2-methylpropiophenone (HMPP) were purchased from Sigma-Aldrich. Penicillin was obtained from Aladdin. All reagents were used without any treatment. The fresh *Premna microphylla* leaves were obtained from local market. The male Sprague-Dawley rats (200 g in weight) were provided by Hangzhou Ziyuan Laboratory Animal Technology Co., Ltd. (Hangzhou, China). All rats were treated following the Laboratory Animal Care and Use Guidelines strictly. All the experimental operations involved in animals were reviewed and approved by the Animal Investigation Ethics Committee of Jinling Hospital.

### 2.2. Characterization

A microscopy (Olympus SZX-16) equipped with a CCD (BioHD-D198) was utilized to capture optical images of CHMN patch. Compression strength of the gels were measured by Universal Testing System (Instron, 68SC-2). SEM images were taken by a scanning electron microscope (SEM, Hitachi SU8010). The UV absorbance was measured by a UV–vis spectrophotometer (Agilent, Cary 5000). Fluorescence images of bacterial and cell staining were captured by a laser scanning confocal microscope (Nikon, A1).

### 2.3. Preparation of plant ash

A preparation method of pure plant origins is as follows: the dry weed *Lolium perenne L.* was collected from local gardens. The weed was burned to ash in a crucible in a windless environment. Then the ash was collected carefully into sample sack.

### 2.4. Sap extraction

10 g of the fresh *Premna microphylla* leaves were first washed with deionized water. Then the leaves were softened by treatment of boiled water for 10 s and rinsed with cold water immediately to avoid destroying chlorophyll. After that, the leaves were kneaded with hand and 150 mL of water was added by several times to obtain a mixture



Fig. 1. Schematic diagram showing the application of CHMN patch derived from the extractives of Chinese herbs for wound healing.

solution. Finally, the solution was filtered by gauze to obtain fresh sap without residue. Additionally, 300, 400, and 500 mL of water was respectively added during the kneading process to acquire sap with different concentration.

### 2.5. Fabrication of the CHMN

The CHMN patch was fabricated according to the process of “Guanyin tofu” in a well-designed silicone mold. AA was mixed into the obtained fresh sap with continuous stirring. After that, the plant ash clear solution dissolved in deionized water and filtered by filter paper was added and mixed thoroughly as coagulator. The mixture was deposited into the MN cavities of silicon mold by centrifuge for 3 min at 5000 rpm. Finally, the mold containing solution was set without move for gelatinization for 30 min. After complete solidification, the CHMN patch was gently detached from the mold for further use. Plant ash solution with original content of 1.5%, 2.0%, 2.5%, and 3.0% was optimized for gelatinization. MN patch was fabricated without the addition of AA. The PEGDA MN patch was fabricated by adding 20% PEGDA solution containing 0.7  $\mu\text{M}$  AA and 1% HMPP into the mold through centrifugation for 3 min at 5000 rpm. After being solidified by UV, the patch was peeled from the mold carefully.

### 2.6. Drug release in vitro

The prepared CHMN patch containing 0.7  $\mu\text{M}$  AA was immersed in 5 mL PBS buffer and kept at 37 °C in a shaker (80r/min). 1 mL of the buffer was collected at 0, 2, 4, 8, 12 and 24 h to record the release of AA, meanwhile equal volume of fresh PBS buffer was supplemented. AA released into the buffer was measured by a UV–vis spectrophotometer. PBS buffer containing 0.7  $\mu\text{M}$  AA was determined as complete release to analyze the release rate of AA from the CHMN patch. MN patches fabricated without AA were utilized for the control experiment to eliminate the interference from the leaf sap. The amount of released AA was calculated by measuring the absorbance values of the CHMN patch hand substrating the MN patch background.

### 2.7. Biocompatibility analysis

The NIH-3T3 cells were cultured in DMEM medium with the addition of 10% FBS and 1% penicillin-streptomycin double antibiotics in an incubator (HERA cell 150, Thermo, USA), 37 °C and 5% CO<sub>2</sub>. The CHMN patches were sterilized by 75% alcohol. Then these patches were rinsed with PBS for 3 times and sterilized by UV light irradiation overnight. 500  $\mu\text{L}$  of NIH-3T3 cell suspension at a concentration of  $0.2 \times 10^5$  cells/mL was co-cultured with the CHMN patches in the 48-well plate (Corning, USA). The cells were observed by the laser scanning confocal microscope through staining with calcein AM. For the MTT assay, 500  $\mu\text{L}$  medium containing 10% MTT was added into the 48-well plate. After 4 h incubation, the liquid was removed and 500  $\mu\text{L}$  of DMSO was added to dissolve the formazan, then the absorbance was measured at 490 nm.

### 2.8. Antibacterial effect in vitro

*Staphylococcus aureus* (*S. aureus*) and *Escherichia coli* (*E. coli*) were cultured in LB medium until the turbidity reached 0.5. Subsequently, the LB medium was replaced by PBS buffer to resuspend the bacteria. The resuspended bacteria were incubated with sterilized CHMN patches for 24 h, respectively. The suspensions were stained by SYTO for 30 min, and then PI for 1 min. 10  $\mu\text{L}$  of the stained suspension was dropped on a slide and covered with a cover glass, then observed under a laser scanning confocal microscope.

### 2.9. Wound healing evaluation

SD rat was first anesthetized and then a circular skin with a diameter

of 1 cm on the back was cut off to create a wound. Subsequently, 100  $\mu\text{L}$  of bacterial suspension was applied to the wound area to establish severe infected wound model. The modeled rats were treated with CHMN patch (CHMN), MN patch without AA (MN), CH patch without microstructure of microneedle (CH), topical administration of VEGF along with penicillin (VEGF), topical administration of AA (AA), PEGDA MN patch containing AA (AA-PEGDA), and PBS solution (control), respectively. Finally, all the treated rats were separated to feed with sufficient water and food. The wound areas were observed and photographed on day 0, 3, 5, 7 and 9 for further analysis. The patches were renewed on the 3rd day after the molding and removed on the 5th day. The topical administration of AA and VEGF was also performed on the 3rd and 5th day. The rats were sacrificed and regenerated tissues were collected on day 9. Each tissue sample was immersed into 4% neutral formaldehyde for fixation.

### 2.10. Histology, immunohistochemistry and immunofluorescence staining

The samples were dehydrated with a series of gradient ethanol after fixation. Then the dehydrated samples were embedded in paraffin and cut into serial sections with thickness of 5  $\mu\text{m}$  for further immunohistochemical analysis. H&E staining and Masson's trichrome staining were used to evaluate epithelization and collagen deposition. IL-6 staining was utilized for immunohistochemistry to evaluate the inflammation. Immunofluorescence staining by primary antibodies against CD31 (KEYGEN, KGYM0118-7) and  $\alpha$ -smooth muscle actin (KEYGEN, KGYT5053-6) were utilized for neovascularization evaluation.

## 3. Results and discussion

In a typical experiment, the CHMN was fabricated by traditional micro-molding technique (Fig. 2a). In brief, the fresh sap from the *Premna microphylla* was obtained after kneading and filtration, which could also be obtained by a juice extractor. Then, AA solution and plant ash solution were added into the sap and completely mixed. Subsequently, the mixed solution was transferred into a silicon mold, followed by a centrifugation treatment to deposit the solution into the microcavities for solidification. After that, the CHMN patch was separated from the mold cautiously for further use. The fabricated CHMN patch possessed a  $20 \times 20$  MN array on a  $15 \times 15$  mm<sup>2</sup> support base (Fig. 2b) and showed verdant owing to the chlorophyll from the leaves (Fig. 2c). The MNs exhibited a cone in shape with the sizes of 300  $\mu\text{m}$ , 5  $\mu\text{m}$  and 600  $\mu\text{m}$  in base diameter, tip diameter and height, respectively, as shown in the scanning electron microscope (SEM) images (Fig. 2d and e).

The sap of the *Premna microphylla* extracted from leaves by hand-made kneading is thick and verdant, which is rich in pectin, various amino acids and proteins (Fig. S1, Supporting Information). The presence of pectin is in favor of increasing the consistency of the sap, which can accelerate the solidification of the solution and enhance the mechanical strength of the obtained “Guanyin tofu” to some extent. Moreover, the addition of coagulator, such as gypsum, calcium carbonate, and plant ash solution can induce the combination of pectin molecules by calcium ion and further controllably manage the solidification time, shape as well as mechanical strength of the desired products (Fig. S2a, Supporting Information). As shown in Fig. S2b, plant ash solution was chosen as “brine” to solidify the sap, which contained calcium ion that could accelerate the sap solidifying (Fig. S2c, Supporting Information). To fabricate the CHMN patch with ideal characteristics, the solidification conditions were first optimized mainly focusing on the water content of the sap and concentration of plant ash. According to the traditional process, different volume of water was added to extract sap from the leaves during kneading. Once solidified by coagulator, all of the gels exhibited stable shape but varying shrinkage degree with the increase of added water after 2 h (Fig. S3a-d, Supporting Information). When the content of fresh leaves was 6.67% according to the traditional

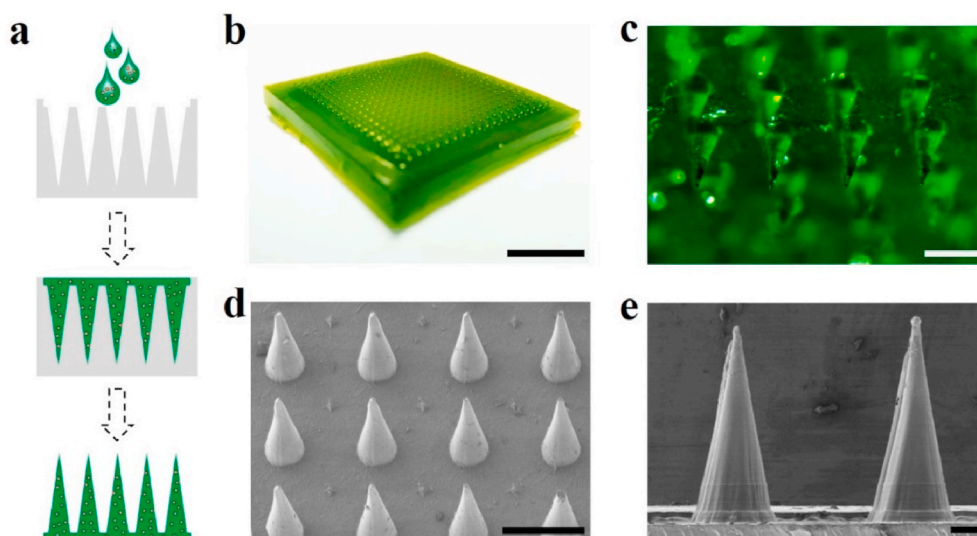


**Fig. 2.** Fabrication and characterization of the CHMN patch: (a) scheme of the fabrication process for CHMN; (b) digital photograph of the CHMN patch; (c) micrograph of the CHMN patch; (d) SEM image of the CHMN; (e) magnified SEM image of the individual MN. Scare bars are 5 mm, 500  $\mu\text{m}$ , 500  $\mu\text{m}$  and 100  $\mu\text{m}$  in (b–e), respectively.

method for preparing “Guanyin tofu”, the gel could maintain its original size. However, when the content decreased to 2%, the gel presented a maximum shrink unable to maintaining the microstructure of MN, which was also analyzed by the upper surface areas of the fabricated gels as shown in Fig. S3e (Supporting Information). Thus, the content of 6.67% was adopted for further research.

Because the binding of pectin molecules is induced by calcium, the concentration of coagulator can have effective impact on the degree of cross-linking, which determines the mechanical strength of the CHMN. Targeting this aspect, different concentrations of plant ash solutions were mixed into the fresh sap for solidification. As shown in Fig. S4a–d (Supporting Information), the gels became fluidity with the decrease of plant ash and even seemed like sol rather than gel when the plant ash concentration was 1.5%. Fig. S4e (Supporting Information) showed the typical stress-strain curves of the gels solidified by different plant ash solution to testify the mechanical strength. The compression strength of the gel was dramatically enhanced from 0.007 MPa solidified by 1.5% plant ash to 0.1 MPa (3.0% plant ash). Further verified in Fig. S5 (Supporting Information), with the addition of low plant ash concentration (1.5%), the gel presented random and dramatically sparse pores after freeze drying owing to the lower cross-linking degree, which indicated the poor mechanical strength. Along with the plant ash concentration increasing from 1.5% to 3.0%, the pores of the gels became increasingly smaller. The phenomenon showed that the cross-linking degree and the mechanical strength of the obtained gels were enhanced with the increasing of the coagulator concentration. Benefiting from the high cross-linking degree and mechanical strength solidified by 3.0% plant ash, the MNs could maintain intact morphology during the fabrication procedure and further applications.

To evaluate the release of active drug AA, 0.7  $\mu\text{M}$  AA was first added in the sap and then solidified into MNs. Then, the CHMN patch was immersed into PBS buffer to verify the release of AA from the CHMN. The relative amount of released AA was measured using a UV–vis spectrophotometer at 0, 2, 4, 8, 12, 24 and 48 h to record the release process. As shown in Fig. S6a (Supporting Information), AA, a kind of pentacyclic triterpenoids, possessed a remarkable absorbance at 211 nm wavelength. Since the sap had a UV absorbance at 211 nm, the AA release was calculated by measuring the absorbance of CHMN patch and subtracting the MN patch background, as shown in Fig. S6b and S6c. The absorbance of the extract solution from the CHMN increased dramatically during the first 12 h after being immersed in PBS buffer, shown in Fig. S6d (Supporting Information). This indicated that AA

could be released from the patch immediately and the sustained release could maintain as long as 24 h. In addition, almost ninety percent of the drugs could be steadily released from the CHMN within 48 h. These features proved the excellent drug load and release capability of the CHMN patch, which possessed the potential to play a significant role in promoting wound healing.

Because of the direct contact between the patches and the wound sites, the biocompatibility is crucially significant for the patches, which can avoid complications caused by the toxic components of the patches. To evaluate the biocompatibility and biosafety of the CHMN path, NIH-3T3 cells were co-cultured with the CHMN patches containing 0.1 (CHMN<sub>1</sub>), 0.3 (CHMN<sub>3</sub>), 0.5 (CHMN<sub>5</sub>) and 0.7  $\mu\text{M}$  (CHMN<sub>7</sub>) AA, respectively. As shown in Fig. 3a and b, Fig. S7a, and S7b (Supporting Information), fluorescence images after staining with calcein AM from 24 to 48 h indicated that the proliferation of 3T3 cells in both experimental groups and control group were fast and the morphology of the cells was also consistent. Furthermore, the cell proliferation rate quantitatively analyzed through using 3-(4,5-dimethylthiazol-2-yl)-2,5-diphenyl tetrazolium bromide (MTT assay) also verified the ideal cell viability co-cultured with CHMN patches (Fig. 3c). The biosafety and biocompatibility of the CHMN was attributed to the use of whole food-grade raw materials. It is worth mentioned that during the entire fabrication process, all of the raw materials were acquired from nature without any complicated chemical processing, which retained the original pharmaceutical activity and avoided the addition of harmful substances. In addition, AA extracted from *Centella asiatica* also had good biocompatibility. These results demonstrated that the fabricated CHMN patch possessed excellent cell biocompatibility for subsequent animal experiments.

AA has been demonstrated its intrinsic inhibitory effects against gram-negative bacterium like *E. coli* and gram-positive bacterium like *S. aureus* as well as fungus. The anti-bacterial activity is attributed to the membrane damage of bacterial caused by AA and the enhanced release of potassium ions and nucleotides sequentially. Herein, the anti-bacterial activity of AA was evaluated by representative bacterial strains of *E. coli* and *S. aureus*. According to previous research, sterilized CHMN patches containing different concentrations of AA were added into the resuspended bacterial solution of *E. coli* and *S. aureus* for co-culture, respectively. After live/dead staining, it could be observed that almost all of the bacteria co-cultured with CHMN<sub>5</sub> and CHMN<sub>7</sub> were died, as shown in Fig. 3d and e, Fig. S7c and S7d (Supporting Information). In addition, statistical analysis certified that almost 100% of

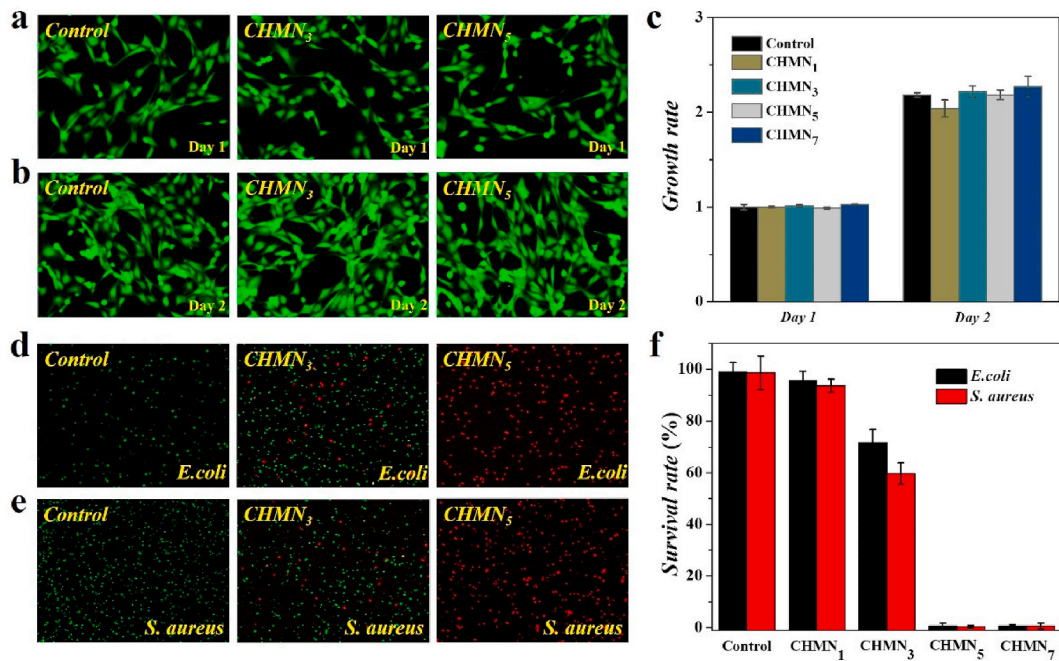


Fig. 3. Biocompatibility and antibacterial assays of the CHMN patch: (a, b) NIH-3T3 cells co-cultured with CHMN<sub>3</sub> and CHMN<sub>5</sub> at day 1 (a) and day 2 (b), cultured in a microplate as control; (c) MTT assay of NIH-3T3 co-cultured with CHMN; (d, e) antibacterial ability of CHMN<sub>3</sub> and CHMN<sub>5</sub> testified by co-culture with *E. coli* (d) and *S. aureus* (e), PBS solution chosen as control; (f) the corresponding statistics of bacterial survival rate.

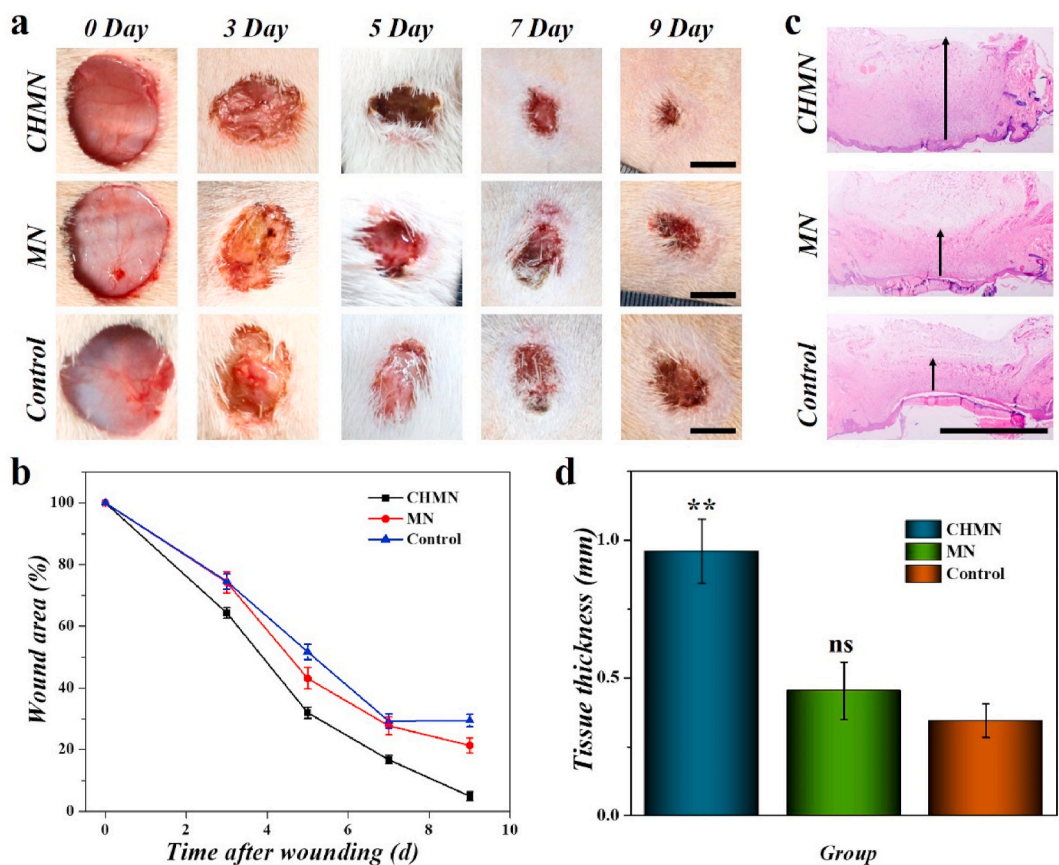


Fig. 4. (a) Representative images of the wounds from day 0 to day 9 with different treatment. (b) Wound repair rate characterized by wound area from day 0 to day 9. (c) H&E staining of wounds with different treatment at day 9. (d) Quantitative analysis of granulation tissue thickness at day 9. \*\* $p < 0.01$ , ns: not significant. Scale bars are 5 mm in (a) and 1 mm in (c), respectively.

both *E. coli* and *S. aureus* were dead (Fig. 3f), which was consistent with the staining results. The bacteria cultured with CHMN<sub>1</sub> showed 96% and 94% survival rate, respectively, while 71% and 60% survival rate of *E. coli* and *S. aureus* was presented with CHMN<sub>3</sub>. On the contrary, bacteria of the control group still survived and maintained normal morphology. Thus, the CHMN containing 0.5 μM AA was selected as wound patch for further use, which exhibited excellent anti-bacterial capability.

In China's ancient times, people usually utilized mashed fresh Chinese herbs or powder of processed Chinese herbs to promote wound healing, which works wonders in the absence of progressive medical technologies. Herein, to verify the efficacy of the CHMN patch in wound healing, infection model was artificially caused by bacteria on the wound areas with 1 cm in diameter on the back of SD rats. CHMN patch and MN patch without AA were subsequently applied onto the wound areas, respectively. As a control, a group of rats were performed with PBS solution. The healing processes of these three groups on day 0, 3, 5, 7 and 9 were recorded for further detailed analysis. As shown in Fig. 4a, in the CHMN group, the wound healing effect was obviously superior to the control group and the MN patch (without AA) group. The area of the wound on day 9 was smallest in the CHMN group and the repair rate was highest (Fig. 4a and b and Fig. S8). The granulation tissue regenerated at the wound area after healing was also analyzed by hematoxylin and eosin (H&E) staining (Fig. 4c and Fig. S9a). Benefited from the excellent repair capability of CHMN, the regenerated granulation tissue could reach  $0.96 \pm 0.12$  mm in thickness which was the maximum among all of the experimental groups; while the granulation tissue thickness of control group was only  $0.35 \pm 0.06$  mm, which indicated the role of AA. Additionally, the thickness of the granulation tissue of the wound treated with normal CH patch without a microneedle structure was  $0.86 \pm 0.10$  mm, which was slightly smaller than the CHMN group (Fig. 4d). The difference might be attributed to the microneedle structure, which was beneficial to cells adhesion, migration as well as gas and substance exchange. In contrast to the groups of patches, the topical administration of both VEGF and AA showed a bit slower rate and thinner granulation tissue. These results demonstrated the efficacy of the drug release capability of the patches. It is worth noting that the MN patch presented an effect of promoting wound healing to some extent comparing the results in AA-PEGDA, MN and control groups. This might

be benefited from the antioxidant compounds in the sap of *Premna microphylla* (Table S1). These results indicated that the CHMN patch exhibited remarkably achievement in the promotion of wound healing and acceleration of granulation tissue regeneration.

As wound infection by bacteria can cause severe complication and even induce death, wound patch is necessarily designed with preventing infection. To demonstrate the performance of the CHMN in preventing infection, expression of interleukin-6 (IL-6) at the wound areas was investigated by immunohistochemistry analysis. IL-6 is a typical proinflammatory factors whose expression can reflect the inflammation level induced by infection at the early stage of the wound healing process. As presented in Fig. 5a and Fig. S10a, IL-6 showed a significantly high expression level in the control group of applying PBS solution, which revealed a severe inflammatory response occurred at the wound site. In the group of MN patch fabricated by sap of *Premna microphylla* only, there was a relatively lower expression of IL-6 compared to the control group, which might resulted from the effect of heat clearing, detoxifying, detumescence and hemostatic of *Premna microphylla*. Remarkably, the expression of IL-6 was downregulated under the treatment containing AA, especially in the CHMN patch group, which was attributed to the intrinsic anti-bacterial property of AA. Benefited from the anti-bacterial effect of the CHMN patch, the wounds could be effectively protected against bacterial infection to avoid severe inflammatory response.

At the last stage of wound repair, the remodeling of skin component is a crucial index of wound healing, which could be intuitively revealed by the deposition of collagen at the site of wound. To evaluate the level of collagen deposition, Masson's trichrome staining was also carried on to certify the wound healing performance. Abundance of collagen stained blue deposited at the wound site in the group treated by the CHMN, as shown in Fig. 5b. The collagen in other groups by different treatments also presented varying degrees of deposition (Fig. S10b). While the control group without effective treatment showed the lowest level of collagen deposition. The skin remodeling evaluated by collagen deposition revealed that the wound healing progress was corresponding to the results of wound closure shown in Fig. 4a. The excellent collagen deposition situation indicated the great potential of CHMN patch for wound-healing.

In addition to collagen deposition, angiogenesis is another necessary

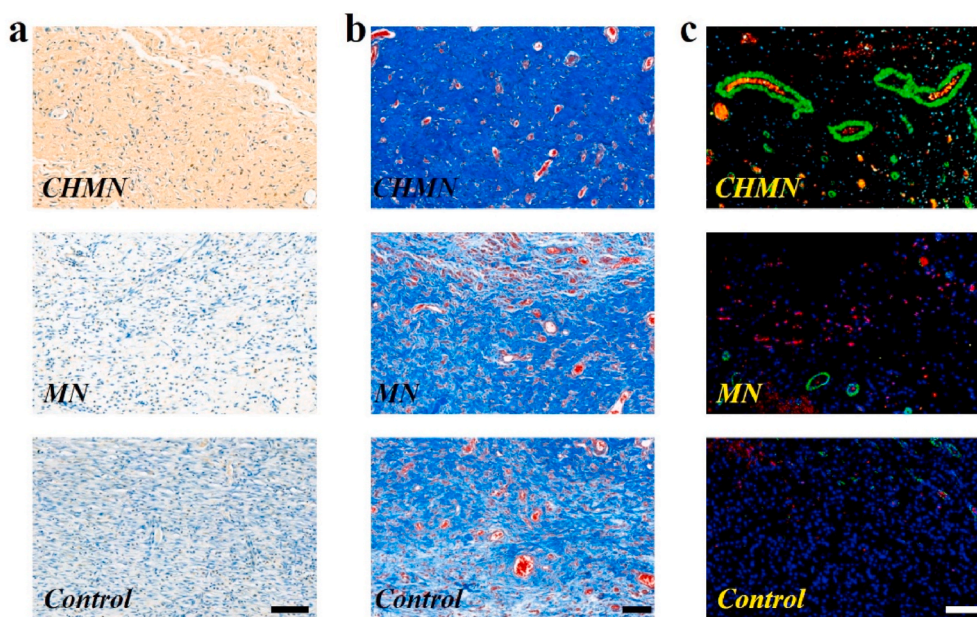


Fig. 5. Characterization of proinflammatory factors, collagen deposition, and neovascularization: (a) immunostaining of IL-6 at granulation tissues in different groups; (b) collagen deposition analyzed by Masson's trichrome staining after 9 days; (d) double immunofluorescence staining (CD31 and  $\alpha$ -SMA) for neovascularization in different groups. Scale bars are 100 μm.

index to assess the skin regeneration. Thus, double immunofluorescence staining of CD31 and  $\alpha$ -smooth muscle actin ( $\alpha$ -SMA), typical markers of the vascular endothelial cell and the vascular smooth muscle cell respectively, were utilized to evaluate the neovascularization at wound sites. In Fig. 5c and Fig. S10c, obvious difference was presented on the density of vascular structure in different groups. The density of positive-stained vessels at the wound site of the CHMN patch treated group was dramatically higher than that in the control group and other treatment groups. The efficient vascular reconstruction was profited from the synergy of AA and *Premna microphylla* where AA played a major role in the acceleration of angiogenesis. This could also be certified by the result presented in the group of MN patch fabricated by *Premna microphylla* solely. In this group, a small quantity of vascular structures was observed, which might be attributed to the limited anti-inflammatory effect of the Chinese herb *Premna microphylla*. In contrast, owing to massive immunocytes aggregated at the wound site induced by bacterial infection, few positive stained vascular structures were observed in the control group (Fig. S11). These results of angiogenesis in the reconstructed skin tissue endowed the CHMN with potential application in wound healing.

#### 4. Conclusion

In summary, we have developed a CHMN patch based on two kinds of traditional Chinese herbs, *Premna microphylla* and *Centella asiatica*, with excellent curative effect for promoting wound healing. The MNs were consisted of the solidified fresh sap of *Premna microphylla* obtained by simple physical method which could not only reserve the activity of the Chinese herb but also eliminate the side effect induced by complicated chemical processing. In addition, with the integration of the AA that extracted from *Centella asiatica*, the CHMN was imparted with an outstanding performance in anti-bacteria, inhibiting inflammatory, collagen deposition, angiogenesis and tissue reconstruction. These features make the CHMN patch great potential for clinical wound healing. Thus, the combination of Chinese herbs and advanced technologies will flourish the development of Chinese herbs and TCM in the modern world.

#### CRedit authorship contribution statement

**Junjie Chi:** conducted experiments and data analysis, Formal analysis, Writing – original draft, wrote the manuscript. **Lingyu Sun:** wrote the manuscript, Writing – original draft. **Lijun Cai:** wrote the manuscript. **Lu Fan:** Writing – original draft, wrote the manuscript. **Changmin Shao:** wrote the manuscript, Writing – original draft. **Luoran Shang:** wrote the manuscript, Writing – original draft. **Yuanjin Zhao:** conceived the idea, designed the experiment, wrote the manuscript, Writing – original draft.

#### Declaration of competing interest

The authors declare no competing financial interests.

#### Acknowledgment

This work was supported by the National Key Research and Development Program of China (2020YFA0908200), the National Natural Science Foundation of China (52073060, 61927805 and 22002018), the Natural Science Foundation of Jiangsu (BE2018707), and the Shenzhen Fundamental Research Program (JCYJ20190813152616459).

#### Appendix A. Supplementary data

Supplementary data to this article can be found online at <https://doi.org/10.1016/j.bioactmat.2021.03.023>.

#### Declaration of interests

The authors declare that they have no known competing financial interests or personal relationships that could have appeared to influence the work reported in this paper.

The authors declare the following financial interests/personal relationships which may be considered as potential competing interests:

#### References

- [1] S. Mahmoudi, E. Mancini, L. Xu, A. Moore, F. Jahanbani, K. Hebestreit, R. Srinivasan, X. Li, K. Devarajan, L. Prelot, C.E. Ang, Y. Shibuya, B.A. Benayoun, A.L.S. Chang, M. Wernig, J. Wysocka, M.T. Longaker, M.P. Snyder, A. Brunet, Heterogeneity in old fibroblasts is linked to variability in reprogramming and wound healing, *Nature* 574 (7779) (2019) 553.
- [2] M.C. Coles, C.D. Buckley, Ready-made cellular plugs heal skin wounds, *Nature* 576 (7789) (2019) 215–216.
- [3] S. Willenborg, S.A. Eming, Cellular networks in wound healing, *Science* 362 (6417) (2018) 891–892.
- [4] G. Chen, Y. Yu, G. Wang, G. Gu, X. Wu, J. Ren, H. Zhang, Y. Zhao, Microfluidic electrospray vitamin metal-organic frameworks encapsulated microcapsules for wound healing, *Research* 2019 (2019) 6175398.
- [5] H. Chen, R. Cheng, X. Zhao, Y. Zhang, A. Tam, Y. Yan, H. Shen, Y.S. Zhang, J. Qi, Y. Feng, L. Liu, G. Pan, W. Cui, L. Deng, An injectable self-healing coordinative hydrogel with antibacterial and angiogenic properties for diabetic skin wound repair, *NPG Asia Mater.* 11 (2019) 3.
- [6] J. He, Y. Qiao, H. Zhang, J. Zhao, W. Li, T. Xie, D. Zhong, Q. Wei, S. Hua, Y. Yu, K. Yao, H.A. Santos, M. Zhou, Gold-silver nanoshells promote wound healing from drug-resistant bacteria infection and enable monitoring via surface-enhanced Raman scattering imaging, *Biomaterials* 234 (2020) 119763.
- [7] L. Shi, X. Liu, W. Wang, L. Jiang, S. Wang, A self-pumping dressing for draining excessive biofluid around wounds, *Adv. Mater.* 31 (5) (2018) 1804187.
- [8] T. Carvalho, G. Guedes, F.L. Sousa, C.S.R. Freire, H.A. Santos, Latest advances on bacterial cellulose-based materials for wound healing, delivery systems, and tissue engineering, *Biotechnol. J.* 14 (12) (2019) 1900059.
- [9] M.A. Shabbazi, M.P.A. Ferreira, H.A. Santos, Landing a lethal blow on bacterial infections: an emerging advance of nanodots for wound healing acceleration, *Nanomedicine* 14 (17) (2019) 2269–2272.
- [10] X. Mao, R. Cheng, H. Zhang, J.H. Bae, L. Cheng, L. Zhang, L. Deng, W. Cui, Y. Zhang, H.A. Santos, X. Sun, Self-healing and injectable hydrogel for matching skin flap regeneration, *Adv. Sci.* 6 (3) (2019) 1801555.
- [11] Z. Liu, Y. Li, W. Li, W. Lian, M. Kemell, S. Hietala, P. Figueiredo, L. Li, E. Makila, M. Ma, J. Salonen, J.T. Hirvonen, D. Liu, H. Zhang, X. Deng, H.A. Santos, Close-loop dynamic nanohybrids on collagen-ark with in situ gelling transformation capability for biomimetic stage-specific diabetic wound healing, *Mater. Horizons* 6 (2) (2019) 385–393.
- [12] J. Chi, X. Zhang, C. Chen, C. Shao, Y. Zhao, Y. Wang, Antibacterial and angiogenic chitosan microneedle array patch for promoting wound healing, *Bioact. Mater.* 5 (2) (2020) 253–259.
- [13] A. Abramson, E. Caffarel-Salvador, V. Soares, D. Minahan, R. Tian, X. Lu, D. Dellal, Y. Gao, S. Kim, J. Wainer, J. Collins, S. Tamang, A. Hayward, T. Yoshitake, H. C. Lee, J. Fujimoto, J. Fels, M.R. Frederiksen, U. Rahbek, N. Roxhed, R. Langer, G. Traverso, A luminal unfolding microneedle injector for oral delivery of macromolecules, *Nat. Med.* 25 (10) (2019) 1512–1518.
- [14] X. Zhang, G. Chen, F. Bian, L. Cai, Y. Zhao, Encoded microneedle arrays for skin interstitial fluid biomarkers detection, *Adv. Mater.* 31 (37) (2019) 1902825.
- [15] M.A. Lopez-Ramirez, F. Soto, C. Wang, R. Rueda, S. Shukla, C. Silva-Lopez, D. Kupor, D.A. McBride, J.K. Pokorski, A. Nourhani, N.F. Steinmetz, N.J. Shah, J. Wang, Built-in active microneedle patch with enhanced autonomous drug delivery, *Adv. Mater.* 32 (1) (2020) 1905740.
- [16] X. Zhang, G. Chen, Y. Yu, L. Sun, Y. Zhao, Bioinspired adhesive and antibacterial microneedles for versatile transdermal drug delivery, *Research* 2020 (2020) 3672120.
- [17] J. Zhu, X. Zhou, H.J. Kim, M. Qu, X. Jiang, K. Lee, L. Ren, Q. Wu, C. Wang, X. Zhu, P. Tebon, S. Zhang, J. Lee, N. Ashammakhi, S. Ahadian, M.R. Dokmeci, Z. Gu, W. Sun, A. Khademhosseini, Gelatin methacryloyl microneedle patches for minimally invasive extraction of skin interstitial fluid, *Small* 16 (16) (2020) 1905910.
- [18] X. Zhang, Y. Yu, G. Chen, L. Sun, Y. Zhao, Bio-inspired clamping microneedle arrays from ferrofluid configured flexible moldings, *Sci. Bull.* 64 (15) (2019) 1110–1117.
- [19] H. Shi, T. Xue, Y. Yang, C. Jiang, S. Huang, Q. Yang, D. Lei, Z. You, T. Jin, F. Wu, Q. Zhao, X. Ye, Microneedle-mediated gene delivery for the treatment of ischemic myocardial disease, *Sci. Adv.* 6 (25) (2020) eaaz3621.
- [20] A. GhavamiNejad, J. Li, B. Lu, L. Zhou, L. Lam, A. Giacca, X. Wu, Glucose-responsive composite microneedle patch for hypoglycemia-triggered delivery of native glucagon, *Adv. Mater.* 31 (30) (2019) 1901051.
- [21] B. Chen, L. Zhang, Y. Xia, X. Zhang, X. Guo, A basal-bolus insulin regimen integrated microneedle patch for intraday postprandial glucose control, *Sci. Adv.* 6 (28) (2020), eaba7260.
- [22] X. Zhang, L. Sun, Y. Yu, F. Bian, Y. Wang, Y. Zhao, Multi-bioinspired slippery surfaces with wettable bump arrays for droplets pumping, *Proc. Natl. Acad. Sci. U. S. A.* 116 (42) (2019) 20863–20868.

- [23] W. Li, J. Tang, R.N. Terry, S. Li, A. Brunie, R.L. Callahan, R.K. Noel, C. A. Rodriguez, S.P. Schwendeman, M.R. Prausnitz, Long-acting reversible contraception by effervescent microneedle patch, *Sci. Adv.* 5 (11) (2019) eaaw8145.
- [24] G. Ying, N. Jiang, S. Maharjan, Y. Yin, R. Chai, X. Cao, J. Yang, A.K. Miri, S. Hassan, Y.S. Zhang, Aqueous two-phase emulsion bioink-enabled 3D bioprinting of porous hydrogels, *Adv. Mater.* 30 (50) (2018) 1805460.
- [25] Y. Li, F. Guo, Y. Hao, S.K. Gupta, J.L. Hu, Y. Wang, N. Wang, Y. Zhao, M. Guo, Helical nanofiber yarn enabling highly stretchable engineered microtissue, *Proc. Natl. Acad. Sci. U. S. A.* 116 (19) (2019) 9245–9250.
- [26] L. Peng, L. Chang, M. Si, J. Lin, Y. Wei, S. Wang, H. Liu, B. Han, L. Jiang, Hydrogel-coated dental device with adhesion-inhibiting and colony-suppressing properties, *ACS Appl. Mater. Interfaces* 12 (8) (2020) 9718–9725.
- [27] K. Zhang, Z. Jia, B. Yang, Q. Feng, X. Xu, W. Yuan, X. Li, X. Chen, L. Duan, D. Wang, L. Bian, Adaptable hydrogels mediate cofactor-assisted activation of biomarker-responsive drug delivery via positive feedback for enhanced tissue regeneration, *Adv. Sci.* 5 (12) (2018) 1800875.
- [28] Q. Feng, J. Xu, K. Zhang, H. Yao, N. Zheng, L. Zheng, J. Wang, K. Wei, X. Xiao, L. Qin, L. Bian, Dynamic and cell-infiltratable hydrogels as injectable carrier of therapeutic cells and drugs for treating challenging bone defects, *ACS Cent. Sci.* 3 (3) (2019) 440–450.
- [29] W. Chen, R. Tian, C. Xu, B. Yung, G. Wang, Y. Liu, Q. Ni, F. Zhang, Z. Zhou, J. Wang, G. Niu, Y. Ma, L. Fu, X. Chen, Microneedle-array patches loaded with dual mineralized protein/peptide particles for type 2 diabetes therapy, *Nat. Commun.* 8 (2017) 1777.
- [30] R. Jamaledin, C.K.Y. Yiu, E.N. Zare, L.N. Niu, R. Vecchione, G. Chen, Z. Gu, F. R. Tay, P. Makvandi, Advances in antimicrobial microneedle patches for combating infections, *Adv. Mater.* 32 (33) (2020) 2002129.
- [31] R. Cheng, L. Liu, Y. Xiang, Y. Lu, L. Deng, H. Zhang, H.A. Santos, W. Cui, Advanced liposome-loaded scaffolds for therapeutic and tissue engineering applications, *Biomaterials* 232 (2020) 119706.
- [32] A. Maxmen, Slew of trials launch to test coronavirus treatments in China, *Nature* 578 (7795) (2020) 347–348.
- [33] D. Cyranoski, The big push for Chinese medicine for the first time, the World Health Organization will recognize traditional medicine in its influential global medical compendium, *Nature* 561 (7724) (2018) 448–450.
- [34] S. Li, Mapping ancient remedies: applying a network approach to traditional Chinese medicine, *Science* 350 (6262) (2015) S72–S74.
- [35] Z. Liu, Chemical insights into ginseng as a resource for natural antioxidants, *Chem. Rev.* 112 (6) (2012) 3329–3355.
- [36] T. Friedemann, M. Li, J. Fei, U. Schumacher, J. Song, S. Schroder, Hypothesis-driven screening of Chinese herbs for compounds that promote neuroprotection, *Science* 350 (6262) (2015) S69–S71.
- [37] Y. Tu, Artemisinin—a gift from traditional Chinese medicine to the world (Nobel Lecture), *Angew. Chem. Int. Ed.* 55 (35) (2016) 10210–10226.
- [38] Y. Han, Y. Jiang, Y. Li, M. Wang, T. Fan, M. Liu, Q. Ke, H. Xu, Z. Yi, An aligned porous electrospun fibrous scaffold with embedded asiatic acid for accelerating diabetic wound healing, *J. Mater. Chem. B* 7 (40) (2019) 6125–6138.
- [39] C. Chang, C. Chen, B. Chen, Y. Su, Y. Chen, M.S. Hershfield, M.T.M. Lee, T. Cheng, Y. Chen, S.R. Roffler, J. Wu, A genome-wide association study identifies a novel susceptibility locus for the immunogenicity of polyethylene glycol, *Nat. Commun.* 8 (2017) 522.
- [40] J. Chen, R. Liang, W. Liu, S. Luo, C. Liu, S. Wu, Z. Wang, Extraction of pectin from *Premna microphylla turcz* leaves and its physicochemical properties, *Carbohydr. Polymers* 102 (2014) 376–384.
- [41] Q. Wu, L. Dong, J. Liu, D. Jiang, Transdermal treatment with Chinese herbal medicine: theory and clinical applications, *Science* 350 (6262) (2015) S82–S83.
- [42] M.H.V. Kumar, Y.K. Gupta, Effect of *Centella asiatica* on cognition and oxidative stress in an intracerebroventricular streptozotocin model of Alzheimer's disease in rats, *Clin. Exp. Pharmacol. Physiol.* 30 (2010) 336–342.
- [43] P. Hashim, H. Sidek, M.H.M. Helan, A. Sabery, U.D. Palanisamy, M. Ilham, Triterpene composition and bioactivities of *Centella asiatica*, *Molecules* 16 (2011) 1310–1322.
- [44] J.T. James, I.A. Dubery, Pentacyclic triterpenoids from the medicinal herb, *Centella asiatica* (L.) Urban, *Molecules* 14 (2009) 3922–3941.